ISSN 1066-3622, Radiochemistry, 2019, Vol. 61, No. 2, pp. 129–136. © Pleiades Publishing, Inc., 2019.
Russian Text © V.N. Serezhkin, M.S. Grigor'ev, A.M. Fedoseev, N.A. Budantseva, L.B. Serezhkina, 2019, published in Radiokhimiya, 2019, Vol. 61, No. 2, pp. 93–99.

Synthesis and Structure of U(VI), Np(VI), and Pu(VI) Phenylacetates

V. N. Serezhkin*[a], M. S. Grigor'ev[b], A. M. Fedoseev[b], N. A. Budantseva[b], and L. B. Serezhkina[a]

[a] *Samara National Research University, ul. Akademika Pavlova 1, Samara, 443011 Russia*
[b] *Frumkin Institute of Physical Chemistry and Electrochemistry, Russian Academy of Sciences,*
Leninskii pr. 31, korp. 4, Moscow, 119071 Russia
**e-mail: Serezhkin@samsu.ru*

Received April 2, 2018; revised May 2, 2018; accepted May 2, 2018

Abstract—Phenylacetates [$AnO_2(C_6H_5CH_2COO)_2$], where An = U (**I**), Np (**II**), or Pu (**III**), were synthesized and studied by single crystal X-ray diffraction. Compounds **I**–**III** are isostructural and crystallize in the monoclinic system, space group $C2/c$, $Z = 4$. The main structural units in crystals of **I**–**III** are 1D chains [$AnO_2\cdot(C_6H_5CH_2COO)_2$] belonging to crystal-chemical group AB^{11}_2 ($A = AnO_2^{2+}$, $B^{11} = C_6H_5CH_2COO^-$). The intermolecular interactions in the structures of [AnO_2L_2] crystals, where L is benzoate or phenylacetate ion, were analyzed by the method of molecular Voronoi–Dirichlet polyhedra. The X-ray structural data were confirmed by analysis of the IR and electronic absorption spectra.

Keywords: uranyl(VI), neptunyl(VI), plutonyl(VI), phenylacetates, actinide contraction, molecular Voronoi–Dirichlet polyhedra

DOI: 10.1134/S1066362219020012

Dicarboxylates $UO_2L_2\cdot nH_2O$ containing anions of monobasic saturated or unsaturated aliphatic acids HL have been studied by now in detail [1]. Much less data are available on uranyl(VI) carboxylates containing anions of monobasic aromatic acids. U(VI) compounds with benzoic acid (hereinafter, Hbox) and some of its halo, hydroxy, and alkyl derivatives have been characterized most extensively. In particular, [$UO_2(box)_2$] was prepared by the reaction of uranyl hydroxide with Hbox at 400 K [2] or of uranyl acetate with Hbox in a water–ethanol mixture [3]. According to [2, 3], in the 1D chain structure of uranyl benzoate crystals the U atoms have coordination number (CN) 6, and all the benzoate ions act as bidentate bridging ligands B^2. Therefore, the uranyl-containing complexes can be described by the crystal-chemical formula AB^2_2, where $A = UO_2^{2+}$ and $B^2 = box^-$. Here and hereinafter, the designations of the ligand coordination types and the crystal-chemical formulas (CCFs) of the complexes are given in accordance with [4, 5]. The reaction of a solution of silver benzoate in ethanol with an aqueous solution of uranyl chloride yielded crystals of [$UO_2(box)_2\cdot(H_2O)$]·EtOH [6]. In their structure, each U atom has CN 7, being bonded with two O atoms of the uranyl ion, two O atoms of bridging anions B^2, two O atoms of the bidentate chelating benzoate ion B^{01}, and the O atom of the water molecule acting as a monodentate terminal ligand M^1. According to [4, 5], two geometric isomers differing in the mutual arrangement (*cis* or *trans*) of the donor atoms of the bridging ligand B^2 in the equatorial plane of the uranyl ion are theoretically possible for complexes with CCF $AB^2B^{01}M^1$. The *trans* isomers form a 1D chain structure; the above-mentioned structure of [$UO_2(box)_2(H_2O)$]·EtOH [6] is an example. On the other hand, the *cis* isomers form a binuclear 0D structure; the known example is [$UO_2(box)_2(Dmfa)$], where Dmfa is dimethylformamide [7, 8]. Some of the characterized benzoate-containing uranyl complexes contain U atoms with CN 8. Mononuclear complexes with CCF AB^{01}_3 in the structure of Na[$UO_2(box)_3$]·$2H_2O$ [9] and centrosymmetrical complexes with CCF $AB^{01}_2M^1_2$ in the crystals of [$UO_2(box)_2(Dmso)_2$], where Dmso is dimethyl sulfoxide [10], can be mentioned as examples.

This study deals with the synthesis and structural characterization of new salts of phenylacetic acid

(Hphac) [$AnO_2(C_6H_5CH_2COO)_2$, An = U (**I**), Np (**II**), Pu (**III**)], which is the second member of the homologous series of monobasic aromatic acids $C_6H_5–(CH_2)_n–COOH$. The structure of only one U(VI) phenylacetate, Na[UO_2(phac)$_3$] [11], has been known by now. There are no data in database [12] on any Np or Pu compounds containing phac ions.

EXPERIMENTAL

Hphac was recrystallized from aqueous solution. To prepare **I**, solid UO_3 calcined at 300°C directly before use was dissolved in an aqueous Hphac solution saturated at 40–50°C. The Hphac : UO_3 molar ratio was (1.2–1.4) : 1. Coarse bright yellow prismatic crystals were formed in the reaction mixture within 1–2 h. In the case of **II** and **III**, the starting substances were $^{237}NpO_2(OH)_2$ and $^{239}PuO_2(OH)_2 \cdot xH_2O$, which were prepared by ozonation of an aqueous suspension of ^{237}Np(VI) and ^{239}Pu(IV) oxalates [13]. The reaction was performed similarly to the synthesis of the uranyl complex, but the reaction mixture temperature was kept below 40°C to avoid reduction of hexavalent Np and Pu. Under these conditions, the side reduction reaction does not affect the growth of the target compound crystals. Salts **II** and **III** are obtained in the form of very thin needle-like crystals, pale green for Np and brownish-yellow for Pu. All the compounds are stable in the solid state for at least several days.

Single crystal X-ray diffraction analysis. The structures of **I–III** were determined by single crystal X-ray diffraction. Measurements were performed with a Bruker Kappa Apex II automatic four-circle diffractometer equipped with an area detector. The unit cell parameters were refined over the whole dataset [14]. The experimental reflection intensities were corrected for absorption using SADABS program [15]. The structures were solved by the direct method (SHELXS97 [16]) and refined by the full-matrix least-squares method (SHELXL-2014 [17]) on F^2 over the whole dataset in the anisotropic approximation for all nonhydrogen atoms. The H atoms of phenylacetate ions were placed in the geometrically calculated positions with the isotropic temperature factors equal to the isotropic factor of the C atom to which they are bonded, multiplied by 1.2. The crystallographic data and parameters of the experiments and refinement of the structures of **I–III** are given in Table 1. The main bond lengths and bond angles and the parameters of hydrogen bonds in the structures of **I–III** are given in Table 2. The CNs of all the atoms were determined by the method of intersecting spheres [18]. The atomic coordinates and thermal parameters are filed at the Cambridge Crystallographic Data Centre, CCDC 1 831 774, 1 831 772, and 1 831 773 for **I**, **II**, and **III**, respectively.

The absorption spectra of the crystalline complexes were measured at room temperature with IR Prestige21 and Shimadzu 3100 spectrophotometers in the ranges 4000–400 cm^{-1} (resolution 2 cm^{-1}, 60 scans) and 400–1300 nm (resolution 1 nm, slit width 1 nm), respectively. Samples for the measurements were prepared by the common procedure: pressing of a finely dispersed mixture of the compound with melted NaCl. The content of the actinide compound in the matrix was about 1% for the IR spectra and 2–10% for the electronic spectra depending on the extinction coefficient of the corresponding actinyl ion.

RESULTS AND DISCUSSION

The X-ray diffraction data show that compounds **I–III** are isostructural. They crystallize in space group *C*2/*c*. The actinide atoms (An = U, Np, or Pu) occupy special positions of C_i symmetry and have CN 8. The coordination polyhedra of the An atoms are hexagonal bipyramids with the oxygen atoms of the actinyl(VI) groups AnO_2^{2+} occupying the apical positions. Six O atoms of four phenylacetate ions are located in the equatorial plane of the AnO_8 bipyramids. The coordination type of each anion is B^{11}, because it is simultaneously bonded with one U atom in the monodentate fashion and with another U atom in the bidentate fashion to form a four-membered ring (Fig. 1). The An=O distances are in the range 1.73–1.75 Å, and the An–O bond lengths in the equatorial plane are in the range 2.42–2.53 Å (Table 2). The main structural units in crystals of **I–III** are electrically neutral 1D [AnO_2· (phac)$_2$] chains having CCF AB_2^{11} (A = AnO_2^{2+}, B^{11} = phac$^-$).

In [AnO_2(phac)$_2$] chains (Fig. 2a) running along [001], the shortest An–An distances are equal to *c*/2, namely: ≈4.24 (**I**), 4.21 (**II**), and 4.20 Å (**III**). In the chains in the above-mentioned structure of [UO_2(box)$_2$] (**IV**) [2, 3] with CCF AB_2^2 (Fig. 2b), the shortest U–U distance in the chain is considerably longer, 5.30 Å (coincides with translation *c*). The more than 1 Å difference between the minimal *d*(An–An) distances in the stoichiometrically similar linear [AnO_2(L)$_2$] chains

Table 1. Crystallographic data and parameters of the experiment and refinement of structures **I**–**III**

Parameter	**I**	**II**	**III**
Chemical formula	$UO_2(C_6H_5CH_2COO)_2$	$NpO_2(C_6H_5CH_2COO)_2$	$PuO_2(C_6H_5CH_2COO)_2$
Crystal system, space group, Z	Monoclinic, $C2/c$, 4	Monoclinic, $C2/c$, 4	Monoclinic, $C2/c$, 4
a, Å	19.6381(4)	19.706(3)	19.7025(7)
b, Å	10.6024(2)	10.3232(18)	10.4028(4)
c, Å	8.4733(1)	8.4158(14)	8.3929(2)
β, deg	102.266(1)	102.127(5)	102.012(2)
V, Å^3	1723.96(5)	1673.8(5)	1682.55(10)
D_x, g cm^{-3}	2.082	2.140	2.149
Radiation, λ, Å	MoK_α, 0.71073	MoK_α, 0.71073	MoK_α, 0.71073
μ, mm^{-1}	9.441	4.036	4.188
T, K	296(2)	100(2)	100(2)
Crystal size, mm	0.24 × 0.14 × 0.06	0.22 × 0.04 × 0.03	0.36 × 0.04 × 0.03
Account of absorption	Semiempirical, by equivalents		
$T_{\min}$, $T_{\max}$	0.344, 0.601	0.635, 0.835	0.775, 0.891
$\theta_{\max}$, deg	34.70	29.98	30.00
Range of h, k, l	$-28 \le h \le 31, -17 \le k \le 16, -13 \le l \le 13$	$-27 \le h \le 27, -14 \le k \le 14, -11 \le l \le 11$	$-27 \le h \le 27, -14 \le k \le 14, -11 \le l \le 11$
Number of reflections: measured/unique (N_1), R_{int}/with $I > 1.96\sigma(I)$ (N_2)	9358/3759, 0.0286/2353	10675/2446, 0.0817/1445	8669/2456, 0.0418/1569
Refinement method	Full-matrix least squares on F^2		
Number of refined parameters	106	106	106
Weight scheme	$w = 1/[\sigma^2(F_o^2) + (0.0107P)^2 + 1.8029P]$, $P = (F_o^2 + 2F_c^2)/3$	$w = 1/[\sigma^2(F_o^2) + (0.0218P)^2$, $P = (F_o^2+2F_c^2)/3$	$w = 1/[\sigma^2(F_o^2) + (0.0112P)^2$, $P = (F_o^2 + 2F_c^2)/3$
wR_2 on N_1	0.0360	0.0711	0.0434
R_1 on N_2	0.0148	0.0300	0.0182
S	0.997	0.984	0.953
$\Delta\rho_{\max}/\Delta\rho_{\min}$, e Å^{-3}	0.610/–0.741	1.968/–1.668	0.780/–1.056

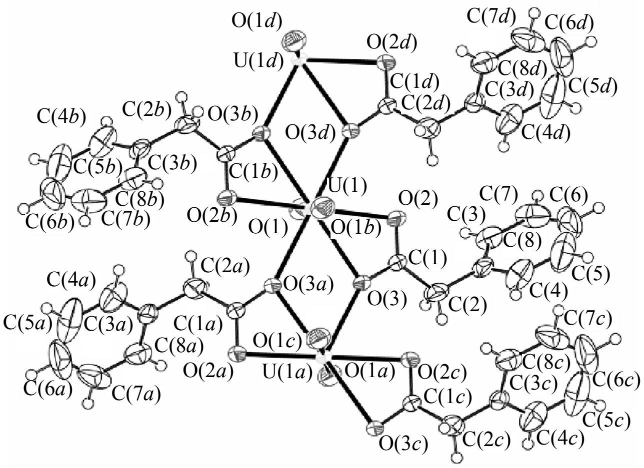

Fig. 1. Structure of the $[UO_2(C_6H_5CH_2COO)_2]$ group in **I** (50% probability ellipsoids).

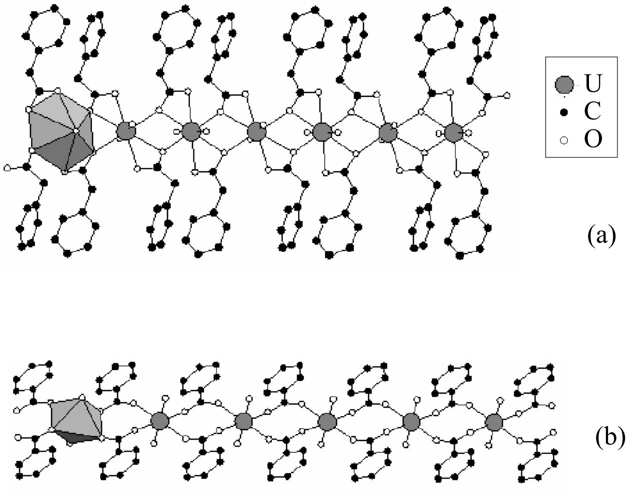

Fig. 2. Fragment of the uranyl carboxylate chain in the crystal structures: (a) $[UO_2(C_6H_5CH_2COO)_2]$ and (b) $[UO_2 \cdot (C_6H_5COO)_2]$. The coordination polyhedron of the U atom is shown to the left. The H atoms are omitted for clarity.

Table 2. Selected bond lengths and bond angles in **I**–**III**

Parameter	**I**	**II**	**III**
AnO_2O_6 hexagonal bipyramid			
Bond	*d*, Å		
An(1)–O(1)	1.7476(18) (×2)	1.737(5) (×2)	1.735(3) (×2)
An(1)–O(2)	2.4940(14) (×2)	2.493(4) (×2)	2.495(3) (×2)
An(1)–O(3)	2.4343(14) (×2)	2.423(4) (×2)	2.419(2) (×2)
An(1)–O(3')	2.5318(13) (×2)	2.505(4) (×2)	2.504(2) (×2)
Angle	ω, deg		
O(1)An(1)O(1)	180.0	180.0	180.0
O(2)An(1)O(3)	70.28(5) (×2)	70.21(13) (×2)	69.91(8) (×2)
O(2)An(1)O(3')	50.78(4) (×2)	51.19(12) (×2)	51.29(8) (×2)
O(3)An(1)O(3')	60.97(6) (×2)	60.85(14) (×2)	61.11(10) (×2)
Phenylacetate ions (coordination type B^{11})			
Bond	*d*, Å		
C(1)–O(2)	1.244(2)	1.238(7)	1.249(4)
C(1)–O(3)	1.282(2)	1.294(7)	1.281(4)
C(1)–C(2)	1.493(3)	1.492(8)	1.508(5)
C(2)–C(3)	1.498(3)	1.499(8)	1.505(5)
C(3)–C(4)	1.365(4)	1.383(9)	1.373(5)
C(4)–C(5)	1.379(6)	1.383(11)	1.371(7)
C(5)–C(6)	1.343(7)	1.361(13)	1.371(7)
C(6)–C(7)	1.356(6)	1.370(12)	1.393(7)
C(7)–C(8)	1.385(4)	1.392(9)	1.384(6)
C(3)–C(8)	1.376(3)	1.370(9)	1.394(5)
Angle	ω, deg		
O(2)C(1)O(3)	117.18(17)	117.0(5)	117.5(3)
O(2)C(1)C(2)	123.27(19)	124.2(6)	122.6(3)
O(3)C(1)C(2)	119.47(18)	118.7(5)	119.6(3)
C(1)C(2)C(3)	115.57(19)	114.5(5)	115.2(3)
C(2)C(3)C(4)	120.1(3)	119.6(6)	120.6(4)
C(2)C(3)C(8)	121.6(3)	122.3(6)	120.2(4)
C(3)C(4)C(5)	120.4(4)	121.5(8)	121.0(4)
C(4)C(5)C(6)	121.3(4)	118.7(8)	120.3(5)
C(5)C(6)C(7)	119.2(4)	121.8(7)	119.9(4)
C(6)C(7)C(8)	120.6(4)	118.4(7)	119.6(4)
C(3)C(8)C(7)	120.2(3)	121.5(6)	120.0(4)
Hydrogen bond parameters			
C(2)–H(2)···O(2) bond [VDP face with RF = 5 [corresponds to the H(2)···O(2) contact][a]			
d[C(2)···O(2)], Å	3.146(3)	3.129(9)	3.151(5)
d[C(2)···H(2)], Å	0.97	0.99	0.99
d[H(2)···O(2)], Å	2.32	2.28	2.32
Ω[H(2)···O(2)], %[b]	17.8	17.9	17.5
C(2)–H(2)···O(2) angle, deg	143	143	141
C(6)–H(5)···O(1) bond [VDP face with RF = 0 [corresponds to the H(5)···O(1) contact][a]			
d[C(6)···O(1)], Å	3.152(4)	3.127(8)	3.125(5)
d[C(6)···H(5)], Å	0.93	0.95	0.95
d[H(5)···O(1)], Å	2.83	2.78	2.79
Ω[H(5)···O(1)], %[b]	12.2	12.8	12.6
C(6)–H(5)···O(1) angle, deg	102	102	102

Table 2. (Contd.)

Parameter	**I**	**II**	**III**
C(7)–H(6)···O(2) [bond [VDP face with RF = 0 [corresponds to the H(6)···O(2) contact][a]			
d[C(7)···O(2)], Å	3.656(4)	3.558(9)	3.552 (5)
d[C(7)···H(6)], Å	0.93	0.95	0.95
d[H(6)···O(2)], Å	2.73	2.61	2.61
Ω[H(6)···O(2)], %[b]	12.3	13.3	13.5
C(7)–H(6)···O(2) angle, deg	174	174	174

[a] RF is the rank of face, i.e., the minimal number of chemical bonds connecting the atoms whose VDPs share a common face. For intermolecular interactions RF = 0, and for intramolecular interactions RF > 1.

[b] Ω is the solid angle (in percents of 4π sr) at which the common face of the Voronoi–Dirichlet polyhedra of the adjacent atoms is seen from the nucleus of any of them.

Table 3. Main parameters of intermolecular interactions in the structures of **I–IV**[a]

Contact A/Z	**I**				**II**				**III**				**IV** [2]			
	k_{AZ}	*d*, Å	S_{AZ}, Å^2	Δ_{AZ}, %	k_{AZ}	*d*, Å	S_{AZ}, Å^2	Δ_{AZ}, %	k_{AZ}	*d*, Å	S_{AZ}, Å^2	Δ_{AZ}, %	k_{AZ}	*d*, Å	S_{AZ}, Å^2	Δ_{AZ}, %
O/O	–	–	–	–	–	–	–	–	–	–	–	–	2	4.37	3.3	1.3
C/O	16	3.15–3.92	7.6	2.3	16	3.13–3.88	7.1	2.1	16	3.13–3.91	7.3	2.2	16	3.77–3.82	7.7	3.0
H/O	52	2.73–5.92	95.5	28.8	52	2.61–5.86	95.1	28.9	52	2.61–5.87	94.3	28.6	72	3.02–4.20	124.6	48.4
C/C	2	3.66	<0.1	<0.1	2	3.54	0.4	0.1	2	3.56	0.3	0.1	76	3.56–4.09	41.6	16.1
H/C	90	2.95–4.26	69.9	21.1	94	2.83–4.67	73.5	22.3	90	2.84–4.16	73.8	22.4	56	3.25–4.02	19.2	7.5
H/H	80	2.64–5.51	158.2	47.8	78	2.53–5.69	153.2	46.5	78	2.56–5.69	154.2	46.7	22	2.45–3.81	61.1	23.7
Total	240	2.64–5.92	331.3	100.0	242	2.53–5.86	329.2	100.0	238	2.56–5.87	329.9	100.0	244	2.45–4.37	257.5	100.0

[a] k_{AZ} is the total number of all the A/Z faces equal to 0 in the molecular VDP per $[AnO_2(L)_2]$ formula unit; *d*, range of the corresponding A–Z interatomic distances; S_{AZ}, total area of all the faces of this type in VDPs of atoms contained in one formula unit of the substance; Δ_{AZ}, partial contribution (in percents) of the corresponding nonvalent A/Z contacts to the integral parameter $^0S = \sum S_{AZ}$ (indicated in the last row) of the molecular VDP.

is caused by the change in the coordination type of the bidentate carboxylate ligand L from B^2 (benzoate ion) to B^{11} (phenylacetate ion), which leads to an increase in CN of uranium from 6 to 8. Despite different CN values of the U atoms, the volume of their Voronoi–Dirichlet polyhedra (V_{vdp}) in the crystals of **I** (9.43 Å^3) and **IV** (9.10 Å^3 [2] or 9.31 Å^3 [3]) coincides within the uncertainty with the mean value of V_{vdp} of U(VI) in UO_n polyhedra [9.3(4) Å^3] at *n* from 5 to 9 [19].

The presence of the methylene bridge $-CH_2-$ in phenylacetate allows easy variation of the steric orientation of the benzene ring due to rotation around the C–C single bond. Whereas in benzoate ions the dihedral angle between the plane passing through the C and O atoms of the carboxy group and the plane of the benzene ring is usually close to 0° because of the conjugation of the π bonds (in **IV** it is ≈13° [3], and in $[UO_2\cdot(box)_2(Dmso)_2]$ [10], ≈5°), in the structure of **I** this angle is ≈66°. In addition, whereas in the $[UO_2(box)_2]$ chains the benzene rings of all the benzoate ions are mutually parallel, in the $[AnO_2(phac)_2]$ chains the mutual orientation of the benzene rings of the adjacent phenylacetate ions is almost perpendicular because of the turn around the C–C bond (in the structures of **I–III**, the corresponding angles are ≈81°, 83°, and 82°, Fig. 2). Different mutual orientation of the adjacent benzene rings in the structures of **I–III** and **IV** influences the features of nonvalent interactions in the crystals, which were analyzed by the method of molecular Voronoi–Dirichlet polyhedra (VDP) [20, 21].

The data obtained show that only five of ten theoretically possible types of intermolecular contacts are realized in the crystal structures of **I–III** (Table 3). The major contribution to binding of $[AnO_2(phac)_2]$ chains is made by H/H dispersion interactions: ≈46–48% of the total area of molecular VDP faces (^0S) corresponding to intermolecular interactions. The second largest contribution is made by C–H···O hydrogen bonds (H/O contacts in Table 3; detailed characteristics of some of them are given in Table 2): partial contribu-

Table 4. Positions of the maxima and possible assignments of the main absorption bands in the IR spectrum of $[UO_2 \cdot (C_6H_5CH_2COO)_2]$

Wavenumber, cm^{-1}	Assignment	Wavenumber, cm^{-1}	Assignment
3070 w, 3036 w	$\nu(CH)_{arom}$	966 m	$\nu_{as}(UO_2)$
2896 w	$\nu(CH)_{aliph}$	944 w	$\nu(C–COO)$
1548 s, 1540 c	$\nu(COO) + \nu(CC)_{arom}$	914 m, 842 w	$\gamma(CH)_{ip}$
1460 s, 1422 m	$\nu(COO) + \delta(CH)$	720 s	$\gamma(CH)_{oop}$
1396 s	$\nu(COO)$	698 m, 668 m	$\delta(COO)$
1336 s	$\omega(CH_2)$	564 m	$\delta(CCC)_{arom}$
1286 s, 1254 m	$\nu(CC)_{arom} + \gamma(CH)_{ip}$	480 w	$\rho(COO)$
1160 w, 1080 w, 1036 w	$\delta(CCC)$		

tion $\Delta_{HO} \approx 29\%$. The contribution of C–H···π interactions (H/C contacts in Table 3) is also significant (≈21–22%). The contribution of the remaining two types of intermolecular contacts, C/O and C/C, to binding of uranyl–anion chains is close to zero: $\Delta \approx 2$ and 0.1%, respectively.

As compared to **I**–**III**, in crystals of **IV** an additional type of dispersion interactions is realized (O/O contacts with $\Delta \approx 1\%$, Table 3). The major contribution to binding of $[UO_2(box)_2]$ chains is made by C–H···O hydrogen bonds, for which $\Delta_{HO} \approx 48\%$, whereas the contribution of H/H dispersion interactions decreases to ≈24%. In contrast to **I**–**III**, π stacking (C/C contacts with $\Delta_{CC} \approx 16\%$) plays a significant role in the structure of **IV**, whereas the contribution of C–H···π interactions is as low as ≈8% (Table 3). The C/O intermolecular interactions in **IV** ($\Delta_{CO} \approx 3\%$), as in **I**–**III**, are insignificant.

In the structures of **I**–**III**, the shortest distance between the centers of the benzene rings (d_{Cg}) is ≈5.1 Å, whereas in **IV** it is 4.06 Å. Therefore, the conclusion on the occurrence of π stacking in **IV** and on its absence in **I**–**III**, based on the results of analysis by the method of molecular VDPs, fully agrees with the criterion $\Delta_{\pi\pi}$ [22], according to which π stacking plays a significant role in organization of the supramolecular architecture of the crystals only if $\Delta_{\pi\pi} = \Delta_{CC} + \Delta_{CN}$ is no less than 2% of ${}^0S$ and d_{Cg} does not exceed 4.1 Å.

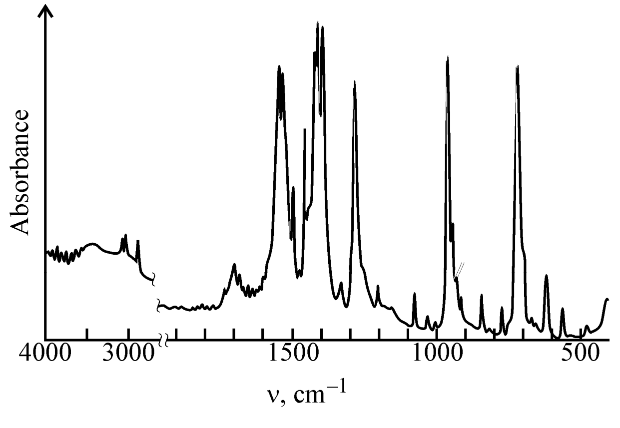

Fig. 3. IR spectrum of $[UO_2(C_6H_5CH_2COO)_2]$ (**I**).

With an increase in the An atomic number in **I**–**III**, actinide contraction is observed. It is accompanied by three effects observed, as a rule, in isostructural An(VI) compounds [23]. For example, in the series U–Np–Pu, the An=O bond length in the AnO_2^{2+} cation regularly decreases (1.748, 1.737, and 1.735 Å, respectively), the volume of the Voronoi–Dirichlet polyhedron of the An atom decreases (9.43, 9.28, and 9.25 $Å^3$), and the dimensionless second moment of inertia of this polyhedron (G_3) increases: 0.083936, 0.083977, and 0.083984, respectively. An increase in G_3 shows that an increase in the number of 5*f* electrons in the series U–Np–Pu is accompanied by a regular decrease in the extent of sphericity of the VDP of the actinide atom.

The IR spectra of **I**–**III** are similar, in accordance with their similar crystal structure. Numerous narrow well-resolved absorption bands of different intensities in the spectra correspond to the vibrations of various functional groups in the compounds. Differences in the positions of the band maxima in going from one compound to another do not exceed several reciprocal centimeters. Figure 3 shows the IR spectrum of $[UO_2(C_6H_5CH_2COO)_2]$. Table 4 presents the wavenumbers of the major absorption band maxima and the band assignments suggested taking into account the known spectrum of the free ligand and the published data [24–27]. A broad weak high-frequency band is due to vibrations of molecular water occluded in the course of the sample preparation. The vibration frequencies of the aromatic ring change only slightly rela-

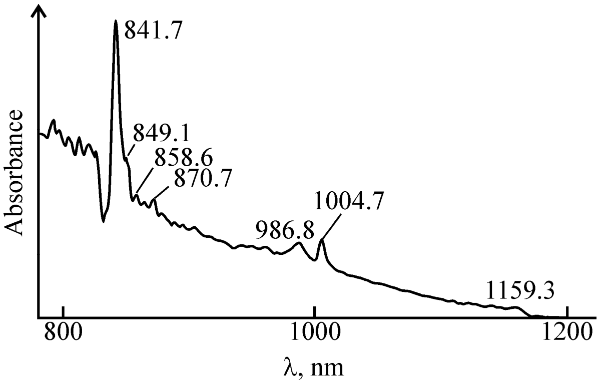

Fig. 4. Fragment of the optical spectrum of $[PuO_2(C_6H_5\cdot CH_2COO)_2]$ (**III**).

tive to the free Hphac. This may be due to the presence of the methylene group shielding the aromatic moiety from the effect of the carboxy group and U atom. As a consequence of coordination of the phenylacetate anion by the uranyl ion, the band of the undissociated Hphac (1765 cm^{-1} for the free ligand) disappears, and stretching vibration bands of the carboxylate ion appear. A strong band at 966 cm^{-1} is assigned to $\nu_{as}(UO_2^{2+})$ stretching vibrations. This frequency is within the range characteristic of uranyl complexes in which the equatorial surrounding consists of O atoms. The $\nu_{as}(AnO_2^{2+})$ frequency only slightly changes in going to Np(VI) and Pu(VI) compounds. This fact correlates with the structural data in accordance with which the An–O interatomic distances in the crystal lattices of **I**–**III** differ only slightly.

The effect of the ligand coordination on the state of the actinyl(VI) group is also manifested in the electronic absorption spectra (near-IR and visible ranges) of the compounds studied, especially in the spectrum of the Pu(VI) complex ($5f^2$ electronic configuration). Figure 4 shows a fragment of the optical spectrum of $[PuO_2(C_6H_5CH_2COO)_2]$, in which there are a narrow strong band of $^3H_4$–$^3H_6$ *f*–*f* electronic transition with the maximum at 841.7 nm and several long-wave satellites. The maximum of the main band is shifted toward longer wavelengths relative to the spectrum of hydrated plutonyl(VI) ion [28]. In the short-wave part of the spectrum, there are weak poorly resolved bands of “uranyl-like” transitions. The calculated extinction coefficient in the maximum of the main absorption band is 230 L mol^{-1} cm^{-1}. The spectrum of $[NpO_2\cdot(C_6H_5CH_2COO)_2]$ is less pronounced; it contains diffuse bands of *f*–*f* electronic transitions from the $^2F_5$ ground state, characteristic of solutions and solid complexes of the NpO_2^{2+} ion ($5f^1$ electronic configuration). The main band is weak (ε = 40 L mol^{-1} cm^{-1}); its maximum at 1228 nm, as in the case of the Pu(VI) complex, is somewhat shifted toward longer wavelengths compared to the spectrum of the hydrated NpO_2^{2+} ion [29].

FUNDING

The study was performed within the framework of the government assignment of the Ministry of Education and Science of the Russian Federation, project 4.5037.2017/8.9. X-ray diffraction experiments were financially supported in part by the Ministry of Science and Higher Education of the Russian Federation (project no. AAAA-A18-118040590105-4).

ACKNOWLEDGMENTS

X-ray diffraction experiments were performed at the Center for Shared Use of Physical Methods of Investigation, Frumkin Institute of Physical Chemistry and Electrochemistry, Russian Academy of Sciences.

CONFLICT OF INTEREST

The authors declare that they have no conflict of interest.

REFERENCES

1. Loiseau, T., Mihalcea, I., Henry, N., and Volkringer, C., *Coord. Chem. Rev.*, 2014, vols. 266–267, pp. 69–109.
2. Cousson, A., Proust, J., Pages, M., et al., *Acta Crystallogr., Sect. C*, 1990, vol. 46, no. 6, pp. 2316–2318.
3. Gao, X., Wang, C., Shi, Z.-F., et al., *Dalton Trans.*, 2015, vol. 44, no. 25, pp. 11562–11571.
4. Serezhkin, V.N., Medvedkov, Ya.A., Serezhkina, L.B., and Pushkin, D.V., *Russ. J. Phys. Chem. A*, 2015, vol. 89, no. 6, pp. 1018–1027.
5. Serezhkin, V.N., Vologzhanina, A.V., Serezhkina, L.B., et al., *Acta Crystallogr., Sect. B*, 2009, Vol. 65, no. 1, pp. 45–53.
6. Nierlich, M., Iroulart, G., Vigner, D., et al., *Acta Crystallogr., Sect. C*, 1990, vol. 46, no. 6, pp. 2459–2460.
7. Navaza, A., Iroulart, M.G., Nierlich, M., et al., *Acta Crystallogr., Sect. C*, 1993, vol. 49, no. 10, pp. 1767–1770.
8. Wang, J.-L., Deng, Z.-Y., Duan, S.-B., and Xing, Y.-H., *J. Coord. Chem.*, 2012, vol. 65, no. 20, pp. 3546–3555.

9. Bismondo, A., Casellato, U., and Graziani, R., *Inorg. Chim. Acta*, 1994, vol. 223, nos. 1–2, pp. 151–153.
10. Shchelokov, R.N., Mikhailov, Yu.N., Orlova, I.M., et al., *Koord. Khim.*, 1985, vol. 11, no. 6, pp. 706–709.
11. Bismondo, A., Casellato, U., Rizzo, L., and Graziani, R., *Inorg. Chim. Acta*, 1992, vol. 191, no. 1, pp. 69–73.
12. *Cambridge Structural Database System*, Cambridge: Cambridge Crystallographic Data Centre, 2017.
13. Fedoseev, A.M., Gogolev, A.V., Shilov, V.P., et al., *Radiochemistry*, 2017, vol. 59, no. 6, pp. 570–578.
14. *SAINT-Plus* (Version 7.68), Madison, Wisconsin (USA): Bruker AXS, 2007.
15. Sheldrick, G.M., *SADABS*, Madison, Wisconsin (USA): Bruker AXS, 2008.
16. Sheldrick, G.M., *Acta Crystallogr., Sect. A*, 2008, vol. 64, no. 1, pp. 112–122.
17. Sheldrick, G.M., *Acta Crystallogr., Sect. C*, 2015, vol. 71, no. 1, pp. 3–8.
18. Serezhkin, V.N., Mikhailov, Yu.N., and Buslaev, Yu.A., *Russ. J. Inorg. Chem.*, 1997, vol. 42, no. 12, pp. 1871–1910.
19. Serezhkin, V.N., *Structural Chemistry of Inorganic Actinide Compounds*, Krivovichev, S.V., Burns, P.C., and Tananaev, I.G., Eds., Amsterdam: Elsevier, 2007, pp. 31–65.
20. Serezhkin, V.N. and Serezhkina, L.B., *Crystallogr. Rep.*, 2012, vol. 57, no. 1, pp. 33–42.
21. Serezhkin, V.N. and Savchenkov, A.V., *Cryst. Growth Des.*, 2015, vol. 15, no. 6, pp. 2878–2882.
22. Novikov, S.A., Peresypkina, E.V., Serezhkina, L.B., et al., *Russ. J. Inorg. Chem.*, 2014, vol. 59, no. 2, pp. 63–71.
23. Serezhkin, V.N., Grigoriev, M.S., Abdulmyanov, A.R., et al., *Inorg. Chem.*, 2017, vol. 56, pp. 7151–7160.
24. Nyquist, R.A. and Settioneri, S.E., *Appl. Spectrosc.*, 1990, vol. 44, no. 10, pp. 1629–1632.
25. Castro, J.L., Lopez Ramırez, M.R., Lopez Tocon, I., and Otero, J.C., *J. Mol. Struct.*, 2003, vols. 651–653, pp. 602–606.
26. Krishnamurthy, M.V., Nagar, M.S., and Hon, N.S., *J. Radioanal. Nucl. Chem.*, 1987, vol. 117, no. 2, pp. 91–98.
27. Lee, H. and Wilmshurst, J.K., *Aust. J. Chem.*, 1969, vol. 22, no. 4, pp. 691–670.
28. Gruen, D.M., *J. Chem. Phys.*, 1952, vol. 20, no. 11, pp. 1818–1821.
29. McGlynn, S.P. and Smith, J.K., *J. Mol. Spectrosc.*, 1961, vol. 6, no. 2, pp. 164–187.

Translated by G. Sidorenko